Performance Evaluation of Intravehicular Activity Spacesuit without the Use of a Liquid Cooling Garment

Monica Mah[1]
NASA-JSC, Houston, TX 77058

Nicholas R. Machak[2]
ASTRION (JETS 2), Houston, TX, 77058

The Orion Crew Survival Systems (OCSS) suit is equipped with safety technology that protects the crew during launch and re-entry and Intravehicular Activities (IVA). It was designed to be used with a Liquid Cooling Garment (LCG), an undergarment with tubes that circulate water to remove excess heat from a crew member. The objective of this study is to determine if the Modified Advanced Crew Escape Suit (MACES), which has very similar material, assembly, and pressure characteristics as the OCSS suit, can be used without the LCG to maintain the crew within their heat storage requirements where exceedances can lead to cognitive and physiological impairment. Testing was completed for both hot and cold environments where test subjects wore varying configurations of the MACES suit ensemble without the LCG. The tests were conducted in a temperature and humidity-controlled chamber with four test subjects ranging from extra small to large. Target metabolic rates were reached using an arm ergometer. To represent the different suit configurations seen in the concept of operations, the suit was tested with visor-down, visor-up, and without helmet and gloves. The test data was analyzed to determine how the environment, test subject size, metabolic rate, and suit configuration affected heat storage. Furthermore, the test data was used to correlate the METMAN model, a transient metabolic man program that simulates the heat transfer within a crew member's body and from a crew member to the surrounding environment. The METMAN correlation showed good agreement between predicted heat storage and test data at the end of the test duration, with a coefficient of determination (R^2) value of 0.8999 for visor-down cases and R^2 of 0.8902 for visor-up and helmet off cases. A correlated METMAN model allows for the analysis and prediction of IVA suit performance without an LCG in additional scenarios.

Acronyms and Nomenclature

ACES	=	Advanced Crew Escape Suits
ACTR	=	Air Cooling Test Rig
CDO	=	Cognitive Deficit Onset
C_{pB}	=	Specific heat capacity of a human
DTO	=	Detailed Test Objective
ECLSS	=	Environmental Control and Life Support System
EMU	=	Extravehicular Mobility Unit
EVA	=	Extravehicular Activity
IVA	=	Intravehicular Activity
JSC	=	Johnson Space Center
L_1	=	Large test subject 1
L_2	=	Large test subject 2
LCG	=	Liquid Cooling Garment
LES	=	Launch Entry Suit

[1] Thermal Analyst, Crew and Thermal Systems Division, 2101 E NASA Parkway, Houston, TX, 77058.
[2] Project Engineer, 2224 Bay Area Blvd, Houston, TX, 77058.

LPO	=	Low-Pressure Outlet
m	=	mass
M_1	=	Medium test subject 1
MACES	=	Modified Advanced Crew Escape Suits
METMAN	=	41 Node Metabolic Man Program
MR	=	Metabolic Rate
NASA	=	National Aeronautics and Space Administration
OCSS	=	Orion Crew Survival Systems
OIG	=	Orthostatic Intolerance Garment
PLSS	=	Portable Life Support System
PGA	=	Pressure Garment Assembly
P_{SAT}	=	Saturation Pressure (psia)
p_v	=	Partial pressure of water vapor (in Hg)
Q_{store}	=	Heat storage
R^2	=	Coefficient of determination
RF	=	radiofrequency
T	=	Temperature
TSAT	=	Saturations Temperature
XS_1	=	Extra small test subject 1

Subscripts

core	=	core
dp	=	dewpoint
ref	=	reference, thermally comfortable temperature
req	=	requirement
skin	=	skin

I. Introduction

THE Liquid Cooling Garment (LCG) has a comprehensive history within the context of human spaceflight at the NASA Johnson Space Center (JSC). Various versions of LCGs have been used with Extravehicular Activity (EVA) suits during the Gemini, Apollo, Skylab, Shuttle and ISS programs as well as Intravehicular Activity (IVA) suits for Shuttle, ISS and Orion programs. These garments are used to control crewmember heat loads. Initially, the Shuttle IVA suit was air-cooled and did not include an LCG. However, after Space Shuttle crewmembers had provided feedback that the Launch Entry Suit (LES) was not providing them with adequate cooling, a liquid cooling garment system was investigated as a solution to keep crewmembers thermally comfortable and prevent them from succumbing to Cognitive Deficit Onset (CDO), heat induced performance degradation. Prior to this, the LES relied solely on the use of a centrifugal blower attached to the suit, supplying 6 ACFM (169.90 lpm) of cabin air through the torso, to provide crewmember cooling [1]. Following ground testing and development, the LCG was integrated and used in the LES starting as a Detailed Test Objective (DTO) with Shuttle mission STS-62 in March 1994. Following the mission, it was formally integrated into the IVA suit architecture on all subsequent Shuttle missions [2].

LCGs are compulsory for some crewed space vehicles based on the extreme thermal environments crewmembers may be exposed to. However, they carry some disadvantages including but not limited to increased cost and schedule for hardware certification and delivery, and increased mass to accommodate a vehicular liquid cooling loop. For crewed vehicles that require IVA suit operations, the exclusion of the LCG from IVA suit architecture and relying solely on air cooling is worth evaluating if those crewmembers are exposed to more benign thermal environments during nominal and contingency operations. The 41Node Metabolic Man Program (METMAN) is a human thermal model that can simulate crew's thermal response given several different environmental and human conditions and can be used to assess feasibility of LCG exclusion within IVA suit architecture. Before these simulations can be run, it is paramount that METMAN be correlated to test data without the use of the LCG, since the model is mostly anchored on test data with test subjects wearing LCGs. Hence, a two-phase study was initiated at NASA JSC. The first phase of this study is a test series involving test subjects wearing IVA suits without LCGs in a thermal chamber. This test series was completed in October 2025, and data from this test series highlighted the performance of the IVA Suit's Pressure Garment Assembly (PGA) in removing excess heat from within the suit at varying metabolic rates. The second phase of this study includes correlating the human thermal model (METMAN) to the test data and updating METMAN intrinsic parameters for the use case of the IVA suit sans an LCG. Model correlation for the helmet visor-down suited configuration was completed in December 2025, and model correlation for the visor-up and helmet & gloves off configurations was completed in February 2026.

II. Test Overview

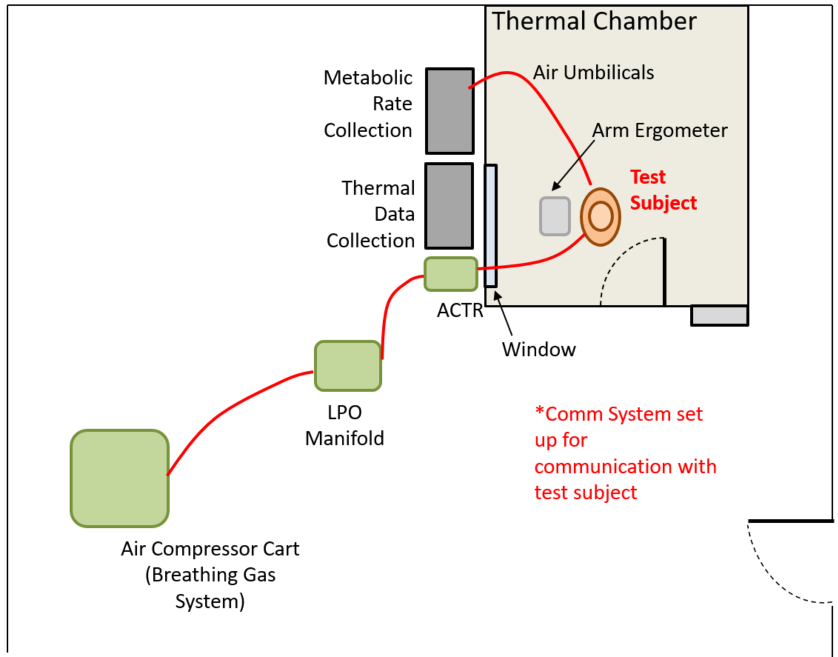

Figure 1. Facility Layout.

The facility layout for the test series is provided in Figure 1. Test subjects donned Modified Advanced Crew Escape Suits (MACES) for this test series. These suits are the same as the Advanced Crew Escape Suits (ACES)—as seen in Figure 2—but were modified to include the same ventilation interfaces that the Orion Crew Survival Systems (OCSS) suit has. The most significant of these modifications was the OCSS ventilation tree that routes breathing gas to the face, as opposed to the back of the head for ACES. The OCSS represents the evolution of the ACES; however, the overall material, assembly, and pressure characteristics remain very similar between the two.

To simulate heat loads and human performance under environmental stress within a crewed cabin, test subjects were directed to operate an arm ergometer located in a temperature- and humidity-controlled thermal chamber. The chamber has a viewing window, allowing test support personnel to observe the test subject during the test series while also allowing test subjects to view the live recording of their metabolic rate on an external monitor. In addition, the chamber has multiple passthroughs to allow for instrumentation wiring to pass out of the chamber and be monitored externally by support personnel. Moreover, there is a passthrough by which the breathing gas provision system umbilical is routed to the suited subject via connection to the suit's Supply Gas Connector. An umbilical delivering the subjects' expired air is additionally routed through a chamber passthrough so that metabolic rate data can be collected by support personnel external to the chamber.

Figure 2. Advanced Crew Escape Suit (ACES).

The breathing gas provision system is comprised of the Breathing Air Compressor Cart, which takes in laboratory air and pressurizes it to a level that is specified by an output regulator and flowmeter. This cart's output is connected to the Low-Pressure Outlet (LPO) Manifold via an umbilical, which further regulates the breathing air pressure down and provides more tuning on air flow rate—to levels of approximately 4.7 ACFM for this test series—passed to the suited test subject. The pressure system connected downstream of the LPO Manifold is the Air Cooling Test Rig (ACTR). This system conditions the air received from the LPO Manifold to the test temperatures and/or test humidities required for assessing the suit's thermal performance. The ACTR is comprised of a heat exchanger, a membrane contactor, and a flowmeter to record the final flow rate into the suit. The main purpose of the heat exchanger is to warm or cool the breathing air to necessary boundary conditions for the test series. The utility fluid to the heat exchanger is provided via a chiller cart, which operates off a 50/50 mix of distilled water and ethylene glycol. The membrane contactor utilizes a microporous hollow fiber membrane, designed to provide a large surface area for water vapor to permeate through and humidify the breathing air. In this application, the breathing air travels outside (shellside), while de-ionized water travels inside (lumenside) the hollow fiber membrane. De-ionized water is looped through the membrane contactor via another chiller cart. The ACTR system has quick-disconnects to easily take the membrane contactor out-of-line for test series boundary conditions where low-humidity is desired.

The instrumentation wiring passing from the test subject to the Thermal Data Collection workstation includes two temperature/humidity probes to record the temperature and humidity of the breathing air entering and exiting the suit. Body core temperature measurements are taken using a sensor-encapsulated pill that moves through the subject's digestive tract and transmits a radiofrequency (RF) signal to an external monitor. Subjects don the monitor during the test series, and a micro-USB cord is routed through the chamber passthrough to the monitor so that the Thermal Data Collection workstation is provided real-time core body temperature data. Lastly, skin temperature measurements are taken. Small iButton temperature sensors provided by iButtonLink, LLC are attached to the subject's body with hypoallergenic adhesive tape. These iButtons are set up to automatically log temperature prior to each test day using a LinkUSBi™ Touch and Hold device connected to the computer at the Thermal Data Collection workstation.

A total of four test subjects were recruited to participate in the test series. The test subjects are referred to with the following identifier: X_Y, where X denotes the suit size of the test subject, and Y is a unique test subject number starting at 1 for each suit size. Hence, the four test subjects for this test series are referred to by the following identifiers: XS_1, M_1, L_1, and L_2.

Table 1 depicts the sets of test points that were conducted as part of the evaluation. The test points are split by test points that would simulate a hot vehicle boundary condition and a cold vehicle boundary condition. Each test point is specified by temperature and humidity set points for the thermal chamber, temperature and humidity target values for the breathing air, and desired metabolic rates from arm ergometer operation (except for Test Point 13, which had test subjects resting in a chair). Subjects performed testing with their helmet visors up, helmet visors down, as well as both helmet and gloves off. Subjects also donned Orthostatic Intolerance Garments (OIGs) for the hot vehicle boundary condition test points, since these garments are nominally worn during dynamic phases of flight to help prevent presyncope effects. The goal time duration for each test point was 45 minutes. The test duration was chosen because it balances achieving steady-state human heat storage levels and avoiding excessive fatigue.

Table 1: Case Matrix

	Test Point	Chamber Temperature [°F]	Chamber Humidity [% rH]	Inlet Breathing Air Temperature [°F]	Inlet Breathing Air Humidity [% rH]	Metabolic Rate [BTU/hr]	Suited Config.
HOT VEHICLE BOUNDARY CONDITIONS	1	86	80*	75	80*	800	OIG donned; visors down
	2	86	80*	75	80*	1200	
	3	86	80*	75	80*	800	OIG donned; visors up
	4	86	80*	75	80*	1200	
	5	86	80*	75	80*	800	OIG donned; helmet and gloves off
	6	86	80*	75	80*	1200	
COLD VEHICLE BOUNDARY CONDITIONS	7	59	20†	55	≤20	600	OIG doffed; visors down
	8	59	20†	55	≤20	800	
	9	59	20†	55	≤20	600	OIG doffed; visors up
	10	59	20†	55	≤20	800	
	11	59	20†	55	≤20	600	OIG doffed; helmet and gloves off
	12	59	20†	55	≤20	800	
	13	59	20†	55	≤20	Resting	OIG doffed; visors up

* Or as high as can be achieved, granted the humidity does not go above 80%.
† Or as low as can be achieved, granted that the humidity does not fall below 20%.

III. Test Results

A. Data Processing to Obtain Heat Storage

The test data aimed to determine if MACES crew members without an LCG stayed within required heat storage limits. For nominal operations, heat storage should remain within the thermal comfort range of - 0.8 to 1.3 BTU/lb (- 1.9 to 3.0 kJ/kg), and for contingency operations, it should be between - 1.8 to 2.0 BTU/lb (- 4.1 to 4.7 kJ/kg), which is the CDO limit. Exceeding these limits can cause discomfort, high body temperatures, CDO, and reduced performance due to overheating. Complex tasks become challenging when heat storage reaches 2.0 BTU/lb (4.7 kJ/kg), which is the upper CDO and contingency operations limit [3].

Heat storage for each test subject is calculated from the temperatures measured by skin temperature sensors and core temperature pill. Equation 1 uses the subject's mass (m), specific heat capacity of the human body (C_{pB}), average skin temperature (T_{skin}), reference skin temperature ($T_{skin_{ref}}$), core temperature (T_{core}) and reference core temperature ($T_{core_{ref}}$) to calculate heat storage (Q_{store}). The reference temperature refers to the thermally comfortable temperature of the test subject, established at the start of each test day while the subject is in shirt sleeves. The difference between thermally comfortable and current temperature represents the change in temperature. If the subject's body temperature has risen relative to initial comfort, this results in a positive ΔT and ΔQ_{store}. Conversely, a cold subject has a lower temperature than the initial comfort level, leading to a negative ΔT and ΔQ_{store}. The skin temperature and core temperature need to be considered to estimate an average body temperature. The formula proposed by Barton in 1935 calculated the mean-body temperature from 64% core temperature and 36% skin temperature. There have been multiple variations of this formula over the years, Snellen suggested an 80% core temperature and 20% skin temperature split for warm environments [4]. This analysis uses an 80% core temperature and 20% skin temperature split based on a heritage use of this equation and previous NASA studies [5]. The skin temperature is averaged, seen in Equation 3. The mass of the test subject is recorded at the beginning of each test day, and the specific heat of a human is 0.839 BTU/lb-°F (3.513 kJ/kg-K) [5]. The requirement for heat storage is written in BTU/lbs. To get heat storage by weight, divide by mass of the test subject, as shown in Equation 2.

$$Q_{store} = m * C_{pB} * (0.2\,(T_{skin} - T_{skin_{ref}}) + 0.8\,(T_{core} - T_{core_{ref}})) \quad (1)$$

$$Q_{store_{req}} = \frac{Q_{store}}{m} \quad (2)$$

The average skin temperature is calculated with an area-weighted average of the temperatures measured at the head (*T1*), chest (*T2*), right thigh (*T3*), shoulder blade (*T4*), right calf (*T5*), left upper arm (*T6*), and left lower arm (*T7*). Figure 3a shows diagram of where the sensors were placed [5].

$$T_{skin} = 0.26 * T1 + 0.06 * T7 + 0.1 * T6 + 0.17 * T3 + 0.15 * T5 + 0.26 * (0.45 * T2 + 0.55 * T4) \quad (3)$$

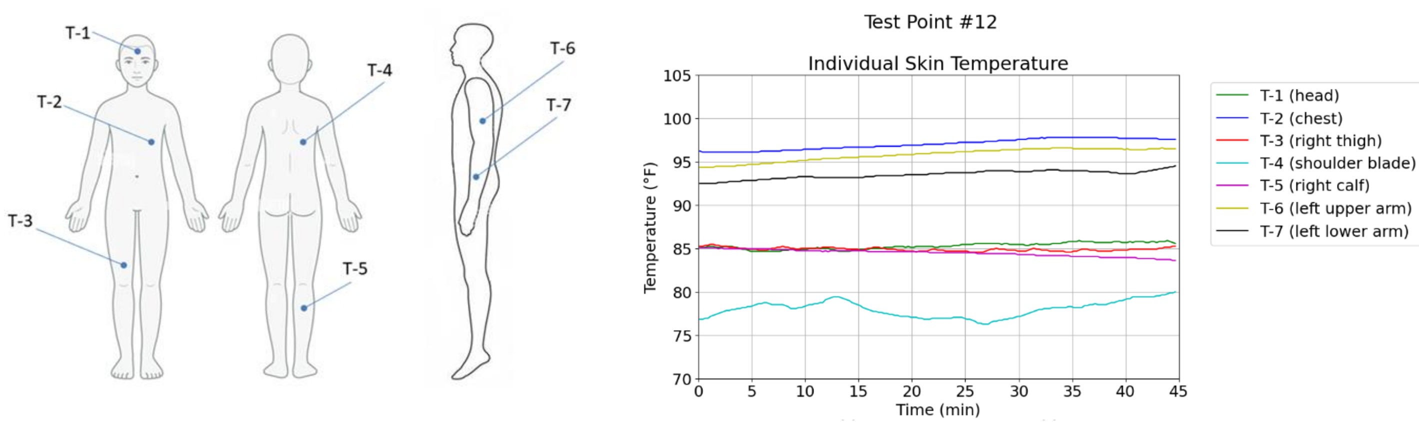

a) Skin Temperature Sensor Locations [6]. b) Lower T-7 Temperature for Subject L_1 during Test Point 12.

Figure 3. Skin Temperature Sensors and Data.

For test subject L_1 during test point 12, the shoulder temperature sensor may have shifted or fallen off since it was showing the temperature of ~77 °F (25 °C) while the rest of the sensors were at 85 – 97 °F (29.4 – 36.1°C), see Figure 3b. The shoulder and chest were assumed to be similar temperature due to their proximity. A modified equation, where only the chest sensor is considered, is used for this case only and is shown in Equation 4.

$$T_{skin} = 0.26 * T1 + 0.06 * T7 + 0.1 * T6 + 0.17 * T3 + 0.15 * T5 + 0.26 * T2 \quad (4)$$

B. Test Data Analysis

The results from the test data are summarized in the Appendix, Table 3 to Table 7. Important metrics to note were the average metabolic rates performed, suit inlet gas temperature, humidity, and flowrate. In the tables, either the minimum or maximum heat storage during that test point is recorded depending on if the maximum was closer to the upper heat storage bound 2.0 BTU/lb (4.7 kJ/kg) or if the minimum was closer to the lower heat storage bound -1.8 BTU/lb (–4.1 kJ/kg). This would give an indication on how close each test was to exceeding the heat storage requirement. It is denoted as the limit heat storage value since it is the discrete heat storage value from the data set that is closest to one of the two the requirement limits. The core temperature and skin temperature with the same timestamp as the limit heat storage value is also recorded. For example, in Table 3 for X_S during test point 3, the maximum heat storage was 2.2 BTU/lb (5.1 kJ/kg), which is over the heat storage requirement upper bound. When the heat storage of 2.2 BTU/lb (5.1 kJ/kg) was reached the corresponding core temperature was 100.5 °F (38.1 °C) and the corresponding skin temperature was 98.4 °F (36.9 °C). Using this on the rest of the data set, the points that reached or exceeded the CDO bounds are test points 3, 4, 6 and 2 for XS_1. The points at or exceeding the comfort limit of -0.8 to 1.3 BTU/lb (–1.9 to 3.0 kJ/kg) are test points 1 and 5 for X_1; test points 2, 4, and 7 for M_1; test points 7, 8, and 11 for L_1; and test points 3, 4, 5, and 11 for L_2. It is important to note that this test data should not be interpreted as true indicators of whether the heat storage requirements are passed or failed during flight. This is because METMAN simulations are ran with a 0 BTU/lb (0 kJ/kg) initial condition for requirement verification, but in practice, test data (including the data cited in this study) rarely starts from zero, making such a condition unrealistic. Thus, the minimum or maximum heat storage value does not indicate whether the air cooling configuration (no LCG) is inadequate to regulate heat. Instead, the goal is to correlate the METMAN model using the non-LCG test data. Using the correlated METMAN model—where the user can set the starting heat storage to 0 BTU/lb (0 kJ/kg) and simulate flight conditions—it can be determined if air cooling maintains acceptable heat storage levels to prevent cognitive impairment.

Figure 4 to Figure **7** display the heat storage for the 45-minute tests, categorized by environment and conditions:

- visor-up with helmets off in hot (test points 3-6) environments
- visor-up with helmets off in cold (test points 9-12) environments
- visor-up, resting in a cold environment (test point 13)
- visor-down in hot (test points 1 and 2) and cold (test points 7 and 8) environments

The visor-up and helmets off cases are categorized together because the chamber and suit airflows can mix in both scenarios. When the subjects are operating the arm ergometer, they deform the suit and initiate airflow exchange for both visor-up and helmet off cases. The resting test point is graphed separately since it does not have a target metabolic rate. The visor-down cases are grouped because there is no air exchange between the cabin and suit.

During testing several interruptions or irregularities were observed including:

- Some test points ended early due to safety limits, such as a subject's heart rate exceeding 85% of the age-predicted maximum for 2 continuous minutes or a core temperature over 100.5 °F. If the heart rate was too high, there was an option to continue the test, but drop down the target metabolic rate by 200 BTU/hr (58.6 W). This can be seen in Table 3 with part A denoting the original goal metabolic rate and part B denoting the reduced metabolic rate. In these test points, the goal metabolic rate dropped from 1200 BTU/hr (351.7 W) to 1000 BTU/hr (293.1 W) for test subject XS_1 at test point 4 and for test subject M_1 at test points 4 and 6. Later, the transient metabolic rates for these changes were captured in the METMAN correlation to make a one-to-one comparison between cases.
- Test points 11 for L_1 and L_2 had data interruptions: the L_1 arm ergometer handle bolt came loose, and the L_2 breathing gas temperature went out of range. Due to the interruption of the test, there is a data gap, and the cold environments graph extends to 60 minutes, although the total testing time adds up to 45 minutes.
- Test Subject L_2 did not complete test points 1, 2, 6, 7, 8, 9, 10, and 12 because they were not local to the test facility area. Additionally on their testing day, there were a few unique test points evaluated that are not included in this paper.

- For test subject L_1 test point 10, the heat storage increases but decreases in the middle of the test. The dip in heat storage comes primarily from a dip in core temperature. The decrease in core temperature is hypothesized to result from the test subject's slower digestion of the core temperature pill, as water intake was shown to inadvertently influence core temperature readings.
- For all test subjects for test points 1, 2, 7, 8 and L_1 for test points 3-6, the skin temperature was sampled at a less frequent time to have enough memory to store the humidity values from the iButton sensors.

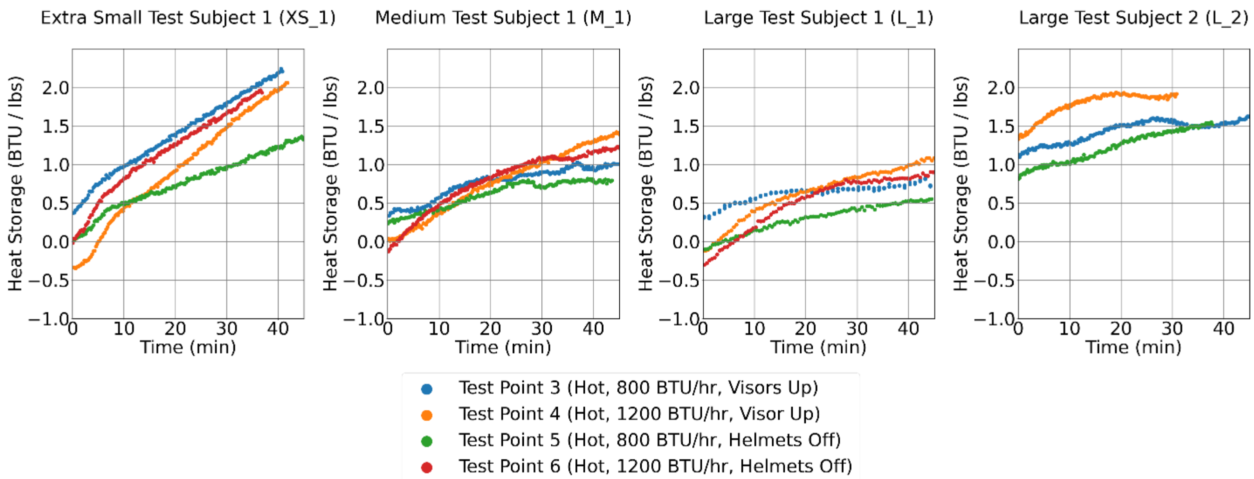

Figure 4. Test Heat Storage Visor-Up and Helmets Off Hot Environment Test Points 3-6.

For Figure 4, which shows the hot, 86 °F (30 °C), visor-up and helmet off test points, the heat storages increase through the 45-minute test period. The slope of increase is highest for the XS_1 test subject. Thermal capacitance significantly affects heat storage differences between varying sized test subjects. Larger subjects, with greater thermal capacitance, take longer to heat up than smaller ones. Another minor impact is that the small subject has a smaller surface body area to dissipate heat through sweating and convection. These were the most strenuous hot cases because there were high metabolic rates in a hot environment. In addition, the visors-up and helmet off cases do not retain all the cool air supplied by the suit.

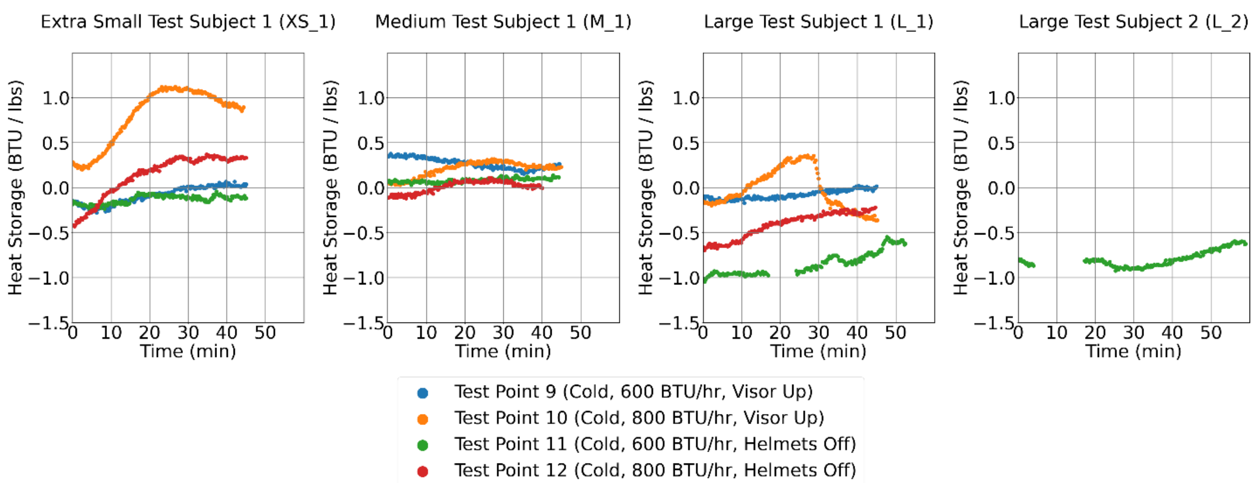

Figure 5. Test Heat Storage Visor-Up and Helmets Off Cold Environment Test Points 9-12.

Figure 5 shows the cold, 59 °F (15 °C), visor-up and helmet off cases (test points 9-12) at 600 BTU/hr (175.8 W) or 800 BTU/hr (234.5 W). For most of the test points, heat storage increases slightly over the 45-minute test. Test subjects were in a cold environment at moderate metabolic rates, which is reasonably comfortable for the test subjects. A more straining cold environment case is resting in a cold environment.

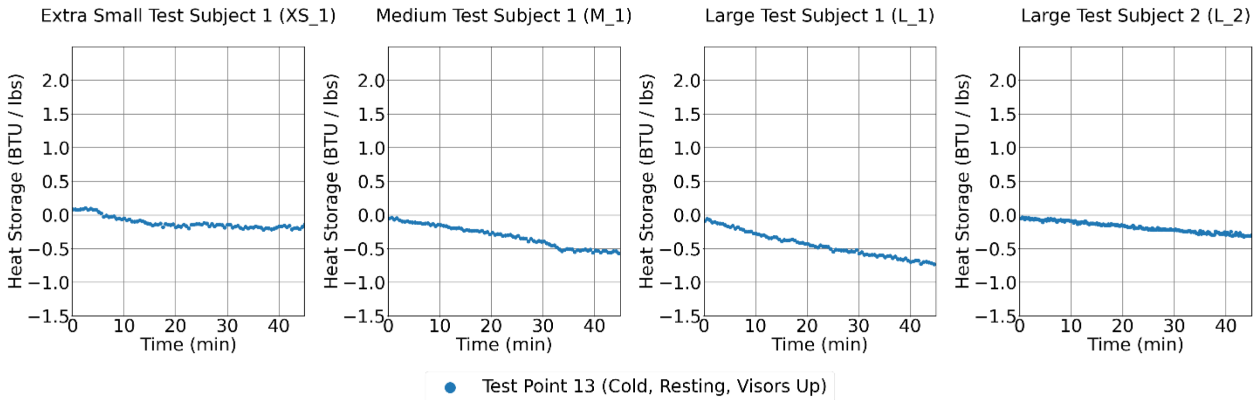

Figure 6. Test Heat Storage Visor-Up, Resting, Cold Environment Test Point 13.

For Figure 6, which shows the resting visor-up cases, the heat storage decreases slowly over the 45-minute test. Here the metabolic rate ranges between 253 BTU/hr - 332 BTU/hr (74.1 – 97.3 W) seen in Table 5. Given that the test subjects are resting with low metabolic rates, their heat storage is understandably negative and decreasing.

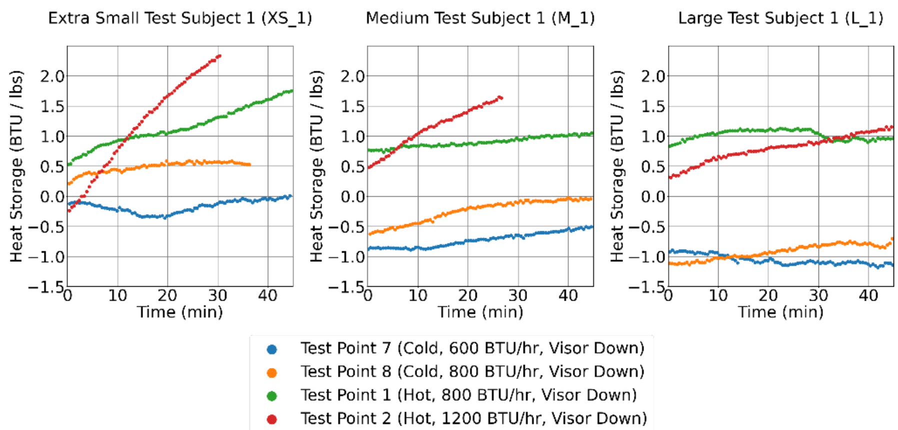

Figure 7. Test Heat Storage Visor-Down Test Points 1, 2, 7, and 8.

For the visor-down cases in Figure 7, the hot test points have higher heat storages than the cold test points. Higher metabolic rates tend towards a larger rate of increase in heat storage. The most extreme heat storage increase occurs in test point 2 when the test subjects are at their highest metabolic rate, 1200 BTU/hr (351.7 W). At higher metabolic rates, the test subjects are working harder, the skin and core temperature increase, which increases heat storage. Most visor-down cold environment cases show a slight increase in heat storage. Test point 7 at 600 BTU/hr (175.8 W) has a decrease in heat storage or is the most unchanged for the test duration. The heat storage is less for visor-down cases as compared to visor-up/helmet off cases because the cool air is contained to the suit.

In summary, larger metabolic rates lead to more heat storage in a shorter amount of time. Hot environments increase heat storage, while cold environments can either increase or decrease heat storage depending on how much activity the test subject is doing, which would mean a higher metabolic rate. The small test subject is more prone to overheating shown in test point 3, 4, 6 and 2 reached or surpassed 2.0 BTU/lb (4.7 kJ/kg).

IV. METMAN Correlation

A. METMAN Overview

METMAN is a human thermal model that simulates the heat transfer and constituent consumption or production of heat within a crew member's body and from a crew member to the surrounding environment. This 41-node Fortran model consists of 10 cylinders that represent the arms, hands, legs, feet, torso, and head. Each of these segments consist of four components: central core, muscle, fat, and skin layer, leading to 40 of the 41 nodes. The last node is the central blood layer [7]. Figure 8 shows a geometric representation of METMAN.

METMAN has four operational modes: Mode 0 - shirtsleeve, Mode 1 - IVA, Mode 2 - EVA, and Mode 3 - helmets off. For this analysis, Mode 1 - IVA was used because it matched the configuration of the visor-down test points. For the visor-up and helmet off cases, Mode 1 – IVA was also used for METMAN, and the airflow rate to the suit was adjusted to account for chamber and suit airflow mixing. Mode 3 - Helmets off is not used for these assessments as Mode 1 showed good correlation to test points, and Mode 3 is based on a flow configuration that is not appropriate and would have required significant work to correct. The types of heat transfer considered were metabolic heat, conduction, sensible heat, radiation, latent heat, and internal convection from blood flow [7].

Heat is produced by converting food into energy and physical activity (metabolic heat). Heat is dissipated through conduction, convection, radiation, and mass transfer to the skin. LCG and air cooling systems can reduce the amount of heat storage and prevent adverse consequences. This analysis examines if air cooling alone is sufficient for IVA operations in the MACES and/or OCCS.

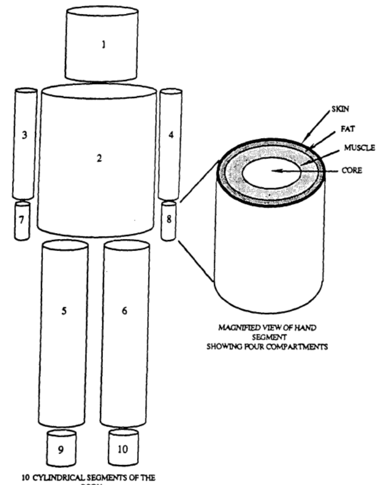

Figure 8. Geometric Representation of METMAN [6].

Table 2. METMAN Body Surface Area

Test Subjects	Weight (lb)	Body Surface Area (ft^2)
M_1, L_2	~170-180	21.3
L_1	~200	24.00
XS_1	~115	15.72

No changes were made to the METMAN code. Only the input values were adjusted, including insulation thickness, body surface area, and test averages such as chamber temperature, chamber dewpoint, suit temperature, suit dewpoint, metabolic rate, and air flow rate. Since there was no LCG, the undergarment insulation thickness was reduced from 0.0141 ft (4.3mm) to 0.00141 ft (0.43mm), which was determined from the visor down cases meeting the heat storage with a lower insulation. The LCG water flow rate was set to 0 to deactivate the LCG. The body surface area for convection is taken from a lookup table with activity level and body size [8]. For this analysis, exercise convection surface areas are used, and the subject's size is based on subject weight. The test subjects and their corresponding weights and body surface area are shown in Table 2. METMAN Body Surface Area. Initial conditions such as metabolic rate, cabin temperature, and suit temperature were adjusted so the test data and METMAN model would start at the same heat storage value. Due to variability in test subject's internal starting conditions (core temperature and skin temperature not aligning perfectly with the thermally comfortable temperatures), the heat storage did not start at 0 BTU/lb (0 kJ/kg). The following inputs were averaged for the test duration then used in METMAN: inlet flowrate into the suit, suit and cabin dewpoint temperature calculated from relative humidity sensors, suit and cabin temperature, wall temperature, and metabolic rate.

B. Visor-Down Configuration

The visor-down configuration is a closed loop because there is no air exchange between the chamber and the suit. This leads to less unknowns since the temperature and humidity are recorded at the suit inlet and outlet air. These visor-down, closed-loop cases are easier to analyze and compare to METMAN because they closely resemble METMAN's current configuration, except for having zero LCG flow and a different insulation thickness to account for the excluded LCG layer. The METMAN correlation for visor-down is shown in Figure 9. This plot graphs the transient METMAN heat storage, demarcated with a line, against the test data, demarcated with a scatter plot. METMAN predicts higher heat storages than the test data for hot environment points, test point 1 and 2. For the hot case, METMAN tends to be conservative, typically predicting that the test subject reaches the upper heat storage limit faster than observed in test data—except at XS_1 test point 1. For the cold environment (test point 7 and 8), there are some instances where the heat storage is higher and some where the heat storage is lower than the test data. Here, METMAN would be conservative if the METMAN predicted heat storage was lower than the test because it would be expected that the cold environment points would reach the lower bound of the heat storage requirement. The transient METMAN and the test data differ because the average test values were used as an input to METMAN. For example, the average metabolic rate is a constant input in METMAN. Every 10 seconds, the test personnel informed the test subject about their metabolic load and whether it was within ±100 BTU/hr (±29.3 W) of the target for that point in the test. Although there were some fluctuations in the test data, the overall heat storage by the end of the test was similar.

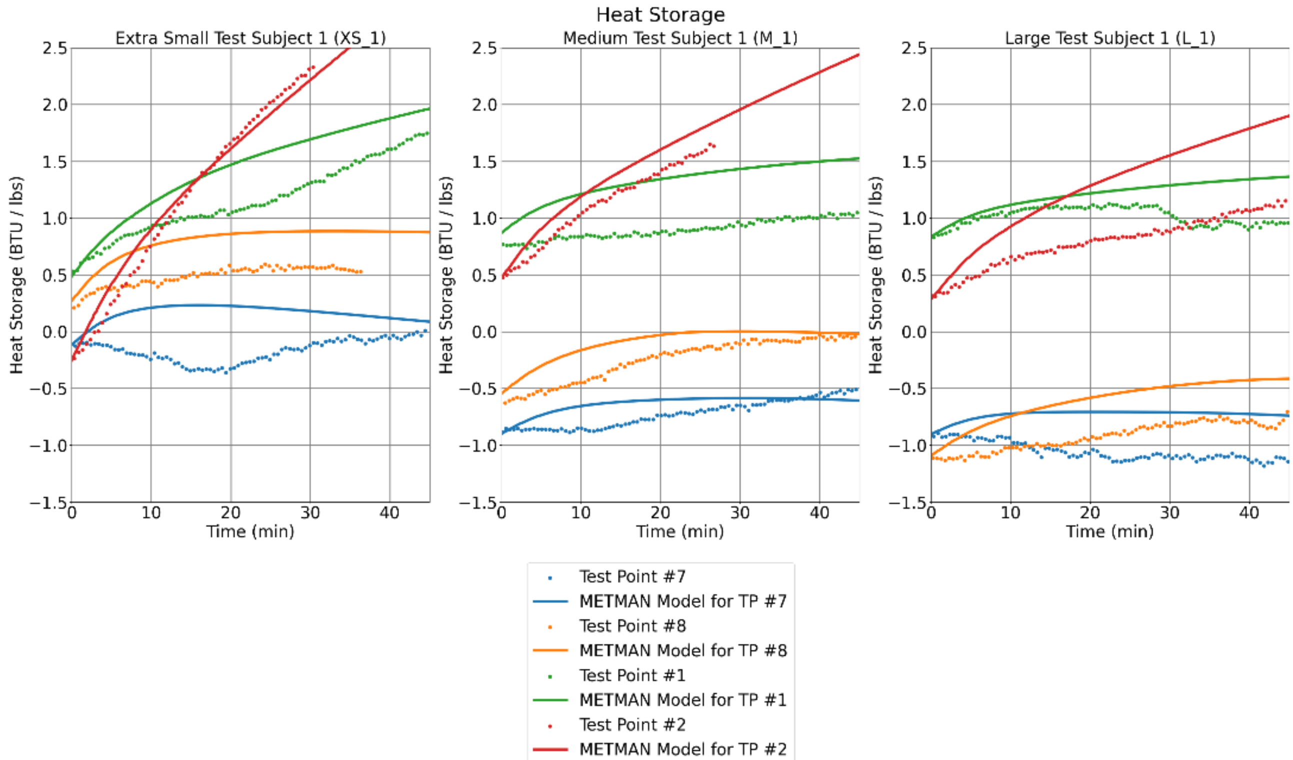

Figure 9. Transient Visor-Down Q_{store} Test vs. METMAN Model.

To examine the heat storage levels from the various test subjects on one graph, the heat storage at the end of the test duration was plotted with the corresponding heat storage from METMAN. The result can be seen in Figure 10, where y = x line represents a perfect correlation. The coefficient of determination (R^2) of the test points relative to the y = x line is 0.8999, which shows good agreement. The data is plotted such that the same configuration is the same color. Lower metabolic rates are demarcated with a circle, and higher metabolic rates are demarcated with a square. METMAN is conservative for test points above the y = x line in the hot environment and for test points below the y = x line in the cold environment.

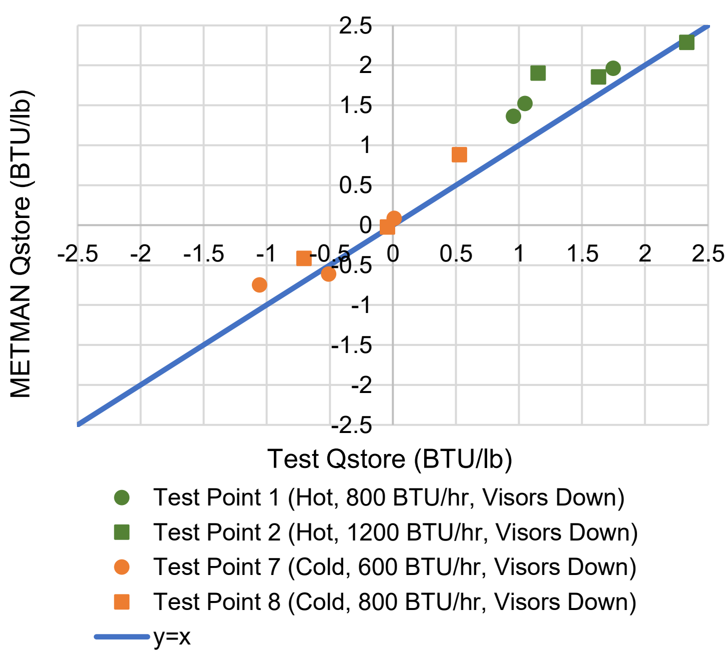

Figure 10. Visor-Down Q_{store} Test vs. METMAN Model at the End of Test Duration.

C. Visor-Up and Helmet Off Configuration

The visor-up and helmet off cases are more challenging to correlate to METMAN than the visor-down cases because there was air exchange between the chamber and the suit at the helmet and gloves that could not be measured. The average cabin temperature, wall temperature, and metabolic rate are inputted to METMAN. The flowrate, suit inlet temperature, and suit dewpoint temperature needed to be adjusted to account for the cabin and suit air mixing. The following paragraphs explain how air mixing is accounted for in each variable.

The primary factor controlling how much airflow entered the suit for visor up or helmet off cases was the person's metabolic rate. The air from the neck ring would escape into the chamber and the suit's movement while using the arm ergometer would cause air exchange between the suit and chamber. Higher metabolic rates would mean more cycles on the arm ergometer, which would mean more air flow between the chamber and suit. For the visor-up, resting cases, there was no air flow since air from the neck ring could go out into the chamber, and there would not be anything to motivate flow to enter the suit. For the high metabolic cases, there is lots of movement and deformations of the suit to maintain the metabolic rate instigating air to travel in and out of the suit.

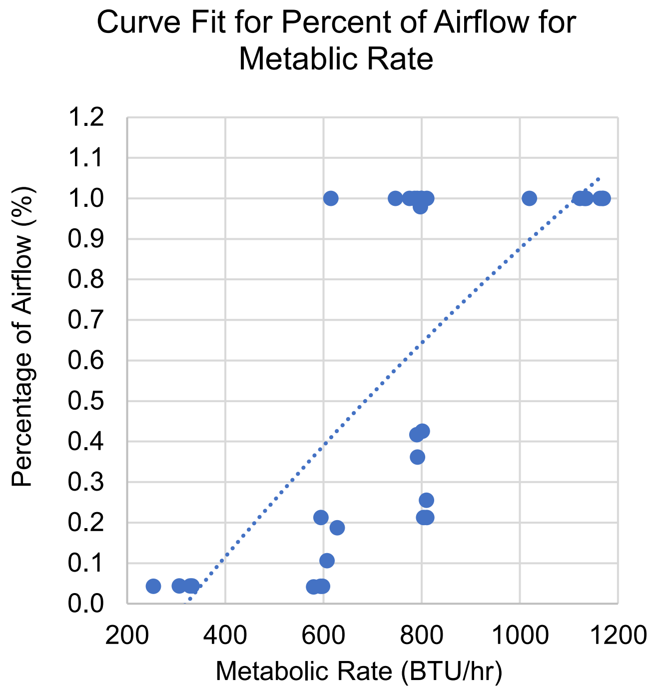

Figure 11. Air Flowrate into Suit Based on Metabolic Rate.

The relationship between airflow exchange and arm movement is demonstrated by plotting the percentage of air flow expected by the metabolic rate (representing the amount of arm movement). To get the percentage of expected flowrate, the suit's inlet airflow model parameter was iteratively decreased for each of these test points until the model and test data differences were minimized. To get the relationship between arm movement and air flow exchange, the percentage of flowrate used for each case was plotted against their corresponding metabolic rate, shown in Figure 11. A second order polynomial curve fit was used to generalize the relationship between air flowrate and metabolic rate, seen in Figure 11 and Equation 5. This is needed in situations where test data is not available and only the metabolic rate is known. The visor-up and helmet off cases were re-ran using the curve fit percentages multiplied by the measured total flowrate.

$$\% \, flowrate = -2.58 * 10^{-7}(MR)^2 + 1.63 * 10^{-3}(MR) - 4.94 * 10^{-1} \quad (5)$$

Since the 1200 BTU/hr (351.7 W) cases were at 100% flowrate due to more arm movements instigating exchange of airflow and the resting cases were at ~ 0% flowrate due to no movement, the curve fit affected the 600 BTU/hr (175.8 W) and 800 BTU/hr (234.5 W) cases the most. The only case that was run at both a hot environment and cold environment was the 800 BTU/hr (234.5 W) metabolic rate and the equation for flowrate had to work for both cold and hot environments. The curve fit tended to be conservative by having lower heat storages for cold cases and higher heat storages for hot cases, as seen in Figure 12.

Since the air is mixing for the visor-up and helmet off cases, the average chamber and suit inlet temperatures are used for the METMAN suit inlet temperature. In addition, the METMAN suit dewpoint is adjusted to the corresponding dewpoint to the average chamber and suit water vapor pressure. Relative humidity of the suit and chamber are measured and can be converted to dewpoint temperatures. The dewpoint temperatures (T_{dp}) use Equation 6 to calculate vapor pressure (P_{SAT} in psia). The chamber and suit vapor pressure (p_v in inHg) is averaged and converted back into dewpoint temperature using Equation 7.

$$P_{SAT} = 0.4912\, e^{\frac{-G-(G^2-4FH)}{2F}} \quad (6)$$

$$F = -7.09 * 10^{-2}$$
$$G = 1.63 * 10^{-3}\,(T_{dp}) - 1.0$$
$$H = -4.29 * 10^{-6}\,(T_{dp})^2 + 3.53 * 10^{-2}(T_{dp}) - 2.52$$

$$T_{dp} = \frac{-G+(G^2-4FH)}{2F} \quad (7)$$

$$F = -4.29 * 10^{-4}$$
$$G = 1.63 * 10^{-3}\,(\ln p_v) + 3.53 * 10^{-2}$$
$$H = (\ln p_v)\,(-7.09 * 10^{-2}\,(\ln p_v) - 1.0) - 2.52$$

Figure 12 shows the visor-up and helmet-off test points (including the resting visor-up test points). It follows the same method of plotting heat storage at the end of the test duration for both the test and METMAN. The R^2 for the visor-up, helmet off, and resting test points relative to the y = x line is 0.8902, which shows good agreement. For most of the test points, METMAN is conservative, where hot environment points are above the y = x line and the cold environment test points are below the y = x line.

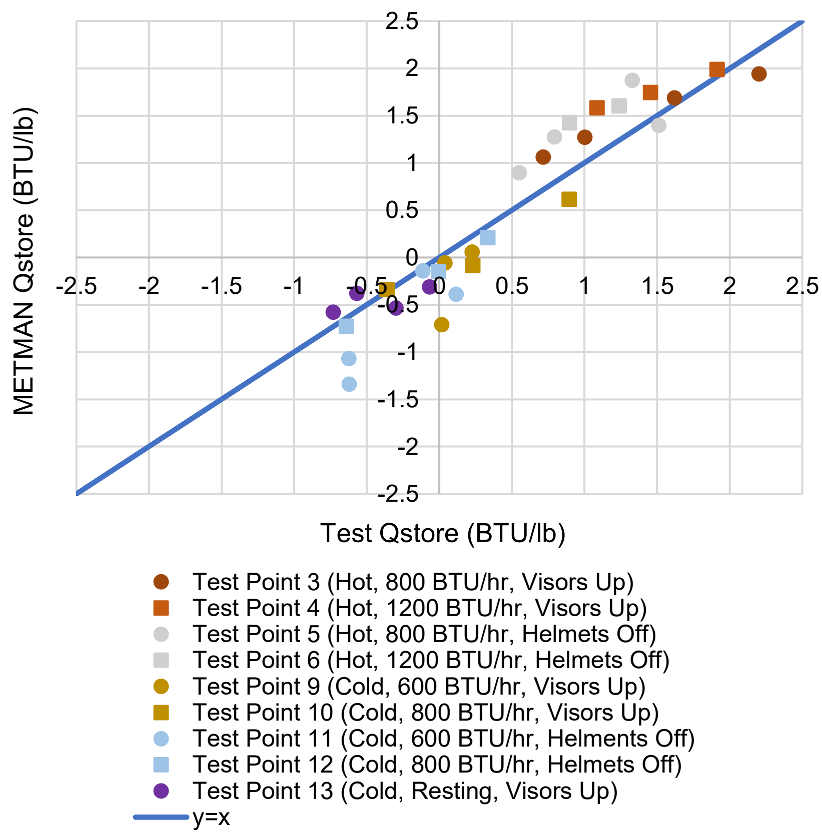

Figure 12. Visor-Up and Helmet Off Q_{store} Test vs. METMAN Model at the End of Test Duration.

V. Conclusion

METMAN model predictions were shown to have good agreement with the test data, as evidenced by the R^2 value of 0.8902 for visors-up and helmet-off configurations per Figure 12 and by the R^2 value of 0.8999 for visors-down configuration per Figure 10. This agreement is significant because despite the differing suited configurations, METMAN base code did not have to be modified to correlate the test data. Only inputs had to be changed to reflect the exclusion of the LCG. This change of inputs included undergarment thickness reduction and LCG water flow rate deactivation.

This study further substantiates METMAN in characterizing IVA Suit Pressure Garment Assembly thermal performance, as well as assessing adherence of crewed vehicles to their pertinent heat storage requirements. The model is even conservative in its predictions, as seen by most hot test points overpredicting heat storage in Figures 10 and 12, as well as the majority of cold test underpredicting heat storage in this figure.

Lastly, it is vitally important to consider multiple suited configurations when assessing vehicle adherence to their crewmember heat storage requirements. As such, the novel approach uncovered in this study of using the percentage of flow rate equation will allow the community to assess crewmember heat storage when in the visors-up and helmet/gloves off suited configurations. Future considerations of this model correlation include conducting more testing to further validate the methodology presented per Equation 5.

Appendix

Table 3: Visor-Up and Helmets Off Test Data for Hot Environments

Test Subject	Test Point	Average Metabolic Rate [BTU/hr]	Limit Core Temp [°F]	Limit Skin Temp [°F]	Limit Heat Storage [BTU/lb]	Average Inlet Breathing Gas Temperature [°F]	Average Flow Rate [ACFM]	Average Inlet Breathing Gas Humidity [%]
XS_1 116.05 lb $T_{core_{ref}}$= 98.89 °F $T_{skin_{ref}}$= 91.51 °F	3	791.3	100.5	98.4	2.2 (max)	74.0	4.7	37.4
	4A[‡]	1162.2	99.7	97.9	1.6 (max)	73.4	4.7	41.0
	4B[‡]	981.0	100.2	98.4	2.1 (max)	73.7	4.7	40.3
	5	791.0	99.5	97.1	1.4 (max)	73.8	4.7	36.8
	6	1163.6	100.3	97.6	2.0 (max)	73.7	4.7	41.8
M_1 175.1 lb $T_{core_{ref}}$= 99.66 °F $T_{skin_{ref}}$= 89.93 °F	3	799.8	99.7	96.1	1.0 (max)	74.6	4.8	39.5
	4A[‡]	1188.1	99.8	96.1	1.1 (max)	74.1	4.8	40.6
	4B[‡]	1007.5	100.2	96.4	1.5 (max)	74.4	4.8	39.3
	5	810.7	99.6	95.1	0.8 (max)	74.1	4.8	40.9
	6A[‡]	1197.6	99.9	95.6	1.1 (max)	74.0	4.8	40.8
	6B[‡]	1001.7	100.1	95.6	1.2 (max)	74.2	4.7	41.1
L_1 See Table 4	3	746.7	98.8	96.1	0.8 (max)	73.9	4.7	56.7
	4	1168.3	99.1	96.7	1.1 (max)	74.0	4.7	55.6
	5	799.0	98.7	94.1	0.5 (max)	74.0	4.7	58.0
	6	1170.2	98.8	95.6	0.9 (max)	74.1	4.6	58.0
L_2 178.8 lb $T_{core_{ref}}$= 99.4 °F $T_{skin_{ref}}$= 84.4 °F	4	1019.4	99.3	96.0	1.3 (max)	73.8	4.7	38.1
	3	775.0	99.5	93.7	1.6 (max)	74.3	4.6	37.4
	5	785.4	99.3	93.9	1.5 (max)	74.1	4.7	49.5

Table 4: Visor-Up and Helmets Off L_1 Weight and Temperatures

Case	Weight [lb]	$T_{core_{ref}}$ [°F]	$T_{skin_{ref}}$ [°F]
L_1 3&4	198.1	98.76	91.54
L_1 5&6	196.7	98.55	91.38

Table 5: Visor-Up, Resting Test Data for Cold Environments

Test Subject	Test Point	Average Metabolic Rate [BTU/hr]	Limit Core Temp [°F]	Limit Skin Temp [°F]	Limit Heat Storage [BTU/lb]	Average Inlet Breathing Gas Temperature [°F]	Average Flow Rate [ACFM]	Average Inlet Breathing Gas Humidity [%]
XS_1	13	253.4	98.9	88.9	-0.2 (min)	56.5	4.7	5.8
M_1	13	328.3	98.7	90.4	-0.6 (min)	55.9	4.6	5.9
L_1	13	332.2[§]	97.7	89.0	-0.7 (min)	55.8	4.6	5.6
L_2	13	306.0	98.7	86.9	-0.3 (min)	55.9	4.6	5.3

[‡] In these test points, the goal metabolic rate dropped from 1200 BTU/hr (351.7 W) in part A to 1000 BTU/hr (293.1 W) in part B because the subject's heart rate exceeding 85% of the age-predicted maximum for 2 continuous minutes. Later, the transient metabolic rates for these changes were captured in the METMAN correlation to make a one-to-one comparison between cases.

[§] Test subject L1's metabolic rate, ventilation, and Tidal Volume were averaged to 190.4 BTU/hr, 6.15 L/min, and 0.41 L, respectively. These values were below what was expected and could have resulted in a leak between the mask and test subject's face. Therefore, an average of the Mifflin-St. Jeor [15] and Harris-Benedict [14] equations were used to calculate expected resting metabolic rate, 332.2 BTU/lb (74.1W). This method was applied to all resting test points. Since there was good agreement with the measured metabolic rate and average of the predicted resting metabolic rate for the other test points, this was deemed an acceptable method for calculating L_1's resting metabolic rate.

Table 6: Visor-Up and Helmets Off Test Data for Cold Environments

Test Subject	Test Point	Average Metabolic Rate [BTU/hr]	Limit Core Temp [°F]	Limit Skin Temp [°F]	Limit Heat Storage [BTU/lb]	Average Inlet Breathing Gas Temperature [°F]	Average Flow Rate [ACFM]	Average Inlet Breathing Gas Humidity [%]
XS_1 115.65 lb $T_{core_{ref}}$ = 99.09 °F $T_{skin_{ref}}$ = 89.01 °F	9	627.9	98.9	88.1	-0.3 (min)	55.4	4.8	5.2
	10	809.7	99.8	93.0	1.1 (max)	55.5	4.7	5.1
	11	614.8	99.1	87.6	-0.2 (min)	55.4	4.8	5.0
	12	801.2	98.7	88.1	-0.4 (min)	55.6	4.7	5.0
M_1 172.00 lb $T_{core_{ref}}$ = 98.89 °F $T_{skin_{ref}}$ = 91.07 °F	9	594.9	99.6	99.6	0.4 (max)	55.8	4.7	5.2
	10	804.1	99.1	90.4	0.0 (min)	55.9	4.7	5.1
	11	606.9	99.5	88.9	0.0 (min)	56.1	4.7	5.1
	12	810.5	99.2	89.1	-0.1 (min)	56.1	4.7	5.0
L_1 207.00 lb $T_{core_{ref}}$ = 98.71 °F $T_{skin_{ref}}$ = 91.46 °F	9	579.9	98.6	89.7	-0.2 (min)	55.3	4.8	5.3
	10	797.5	98.3	90.1	-0.4 (min)	55.3	4.8	5.2
	11	594.3	97.7	88.4	-1.0 (min)	55.7	4.7	5.1
	12	790.1	98.0	89.3	-0.7 (min)	55.5	4.8	5.0
L_2 178.2 lb $T_{core_{ref}}$ = 98.9 °F $T_{skin_{ref}}$ = 88 °F	11	598.1	98.2	85.5	-0.9 (min)	55.4	4.7	5.3

Table 7: Visor-Down Test Data for Hot and Cold Environments

Test Subject	Test Point	Average Metabolic Rate [BTU/hr]	Limit Core Temp [°F]	Limit Skin Temp [°F]	Limit Heat Storage [BTU/lb]	Average Inlet Breathing Gas Temperature [°F]	Average Flow Rate [ACFM]	Average Inlet Breathing Gas Humidity [%]
XS_1 115.65 lb $T_{core_{ref}}$ = 99.09 °F $T_{skin_{ref}}$ = 89.01 °F	7	615.7	98.7	88.9	-0.4 (min)	56.0	4.7	5.8
	8	813.5	99.6	91.1	0.6 (max)	56.1	4.7	5.7
	1	805.4	99.8	97	1.7 (max)	73.8	4.7	56.2
	2	1151	100.4	98.3	2.3 (max)	73.8	4.7	56.1
M_1 172.00 lb $T_{core_{ref}}$ = 98.89 °F $T_{skin_{ref}}$ = 91.07 °F	7	609.4	98.4	89.5	-0.9 (min)	56.1	4.7	5.8
	8	811.8	98.6	90.5	-0.6 (min)	56.3	4.7	5.7
	1	797.5	99.8	95.5	1.0 (max)	74.6	4.6	57.4
	2	1214.3	100.3	97.3	1.7 (max)	74.4	4.7	54.9
L_1 207.00 lb $T_{core_{ref}}$ = 98.71 °F $T_{skin_{ref}}$ = 91.46 °F	7	590.6	97.2	88.5	-1.2 (min)	56.0	4.7	5.3
	8	782.3	97.1	89	-1.1 (min)	56.3	4.7	5.2
	1	776	98.7	96.1	1.1 (max)	73.9	4.6	53
	2	1173.5	99.1	96.2	1.2 (max)	74.8	4.7	55

Acknowledgments

The authors would like to thank Kirstyn Johnson (NASA JSC) and Bruce Conger (Amentum) for their feedback and technical guidance. The authors would like to thank Bruno Miranda for running METMAN cases for model correlation. The authors would also like to thank the members on the Crew Survival Engineering team and the team members on the Human Health and Performance Contract 2 (HHPC2) contract for their contributions.

References

[1] C.-M. Chang, B. W. Sauser, G. C. Bue and B. C. Conger, "Space Shuttle Launch Entry Suit Thermal Performance Evaluation," *SAE Transactions,* vol. 102, pp. 1646-1659, 1993.

[2] G. C. Bue, M. K. Ewert, C. H. Lin and S. V. Walker, "Launch Entry Suit Individual Cooling Unit Thermal Qualification Test Report," NASA Johnson Space Center, Houston, TX, 1997.

[3] "MPCV 70024 Orion Multi-Purpose Crew Vehicle Program: Human Systems Integration Requirements (HSIR)," NASA, 4 March 2015.

[4] R. L. a. D. I. Sessler, "Estimation of Mean-body Temperature From Mean-skin and Core Temperature," *Anesthesiology,* vol. 105, no. 5, pp. 1117-21, 2006.

[5] B. Miranda, "METMAN Analysis of FY19 OCSS LCG Testing," NASA, Houston, October 10, 2019.

[6] "Human Body Outline Front And Back Unisex," [Online]. Available: https://animalia-life.club/qa/pictures/human-body-outline-front-and-back-unisex. [Accessed 2 February 2026].

[7] G. C. Blue, "Computer Program Documentation 41-Node Transient Metabolic Man Program," NASA, Houston, 1989.

[8] M. Ewert, "Human Metabolic Modeling Updates," NASA, Houston, April 2, 2020.

[9] G. H. Vatistas, S. Lin and C. K. Kwok, "Reverse Flow Radius in Vortex Chambers," *AIAA Journal,* vol. 24, no. 11, pp. 1872-1873, 1986.

[10] R. Peyret and T. D. Taylor, Computational Methods in Fluid Flow, 2nd ed, Chapters 7, 14., New York: Springer-Verlag, 1983.

[11] F. J. Guerrero-Gonzalez, P. Reiss, M. L. Donten, A. Lovagnini and L. Celiento, "Low-temperature Molten Salt Electrolysis for Lunar Regolith Reduction," in *54th International Conference on Environmental Systems*, Prague, Czechia, ICES-2025-441, 2025.

[12] C. J. Nietubicz, J. E. Heavey and J. L. J. Steger, "A General Curvilinear Grid Generation Program for Projectile Configurations," U.S. Army Ballistic Research Lab., Rept. ARBRL-MR03142, Aberdeen Proving Ground, MD, Oct. 1981.

[13] A. Vickers, ""10-110 mm/hr Hypodermic Gravity Design A," Rainfall Simulation Database," [Online]. Available: http://www.geog.le.ac.uk/bgrg/lab.htm. [Accessed 15 March 1998].

[14] S. E. Jacobs, D. Green, D. B. Tufts and D. Gohmert, "Development of a Custom Space Suit for Orion," in *49th International Conference on Environmental Systems*, Boston, Massachusetts, 2019.

[15] A. M. a. H. M. S. Roza, "The Harris Benedict equation reevaluated: resting energy requirements and the body cell mass.," *The American journal of clinical nutrition,* vol. 40, no. 1, pp. 168-82, 1984.

[16] M. D. S. J. S. T. H. L. A. S. B. J. D. S. A. &. K. Y. O. Mifflin, " A new predictive equation for resting energy expenditure in healthy individuals," *The American journal of clinical nutrition,* vol. 51, no. 2, pp. 241-247, 1990.